

# Type I Interferons Control Proliferation and Function of the Intestinal Epithelium

Yuliya V. Katlinskaya,<sup>a</sup> Kanstantsin V. Katlinski,<sup>a</sup> Audrey Lasri,<sup>b</sup> Ning Li,<sup>a</sup> Daniel P. Beiting,<sup>c</sup> Amy C. Durham,<sup>c</sup> Ting Yang,<sup>d</sup> Eli Pikarsky,<sup>e</sup> Christopher J. Lengner,<sup>a</sup> F. Brad Johnson,<sup>d</sup> Yinon Ben-Neriah,<sup>b</sup> Serge Y. Fuchs<sup>a</sup>

Department of Biomedical Sciences, School of Veterinary Medicine, University of Pennsylvania, Philadelphia, Pennsylvania, USA<sup>a</sup>; The Lautenberg Center for Immunology and Cancer Research, IMRIC, Hebrew University-Hadassah Medical School, Jerusalem, Israel<sup>b</sup>; Department of Pathobiology, School of Veterinary Medicine, University of Pennsylvania, Philadelphia, Pennsylvania, USA<sup>c</sup>; Department of Pathology and Laboratory Medicine, Perelman School of Medicine, University of Pennsylvania, Philadelphia, Pennsylvania, USA<sup>d</sup>; Department of Pathology, Hebrew University-Hadassah Medical School, Jerusalem, Israel<sup>e</sup>

**Wnt pathway-driven proliferation and renewal of the intestinal epithelium must be tightly controlled to prevent development of cancer and barrier dysfunction. Although type I interferons (IFN) produced in the gut under the influence of microbiota are known for their antiproliferative effects, the role of these cytokines in regulating intestinal epithelial cell renewal is largely unknown. Here we report a novel role for IFN in the context of intestinal knockout of casein kinase 1 $\alpha$  (CK1 $\alpha$ ), which controls the ubiquitination and degradation of both  $\beta$ -catenin and the IFNAR1 chain of the IFN receptor. Ablation of CK1 $\alpha$  leads to the activation of both  $\beta$ -catenin and IFN pathways and prevents the unlimited proliferation of intestinal epithelial cells despite constitutive  $\beta$ -catenin activity. IFN signaling contributes to the activation of the p53 pathway and the appearance of apoptotic and senescence markers in the CK1 $\alpha$ -deficient gut. Concurrent genetic ablation of CK1 $\alpha$  and IFNAR1 leads to intestinal hyperplasia, robust attenuation of apoptosis, and rapid and lethal loss of barrier function. These data indicate that IFN play an important role in controlling the proliferation and function of the intestinal epithelium in the context of  $\beta$ -catenin activation.**

The mature mammalian gut epithelial lining requires continuous cell proliferation that enables the replacement of lost cells and almost weekly tissue renewal (1). This renewal driven by the Wnt- $\beta$ -catenin pathway must be tightly controlled to ensure the proper differentiation of intestinal epithelial cells (IECs). IEC differentiation is required to maintain normal intestinal functions and to prevent the development of colorectal cancers (2, 3). Development of these cancers often depends on the interaction of the host with commensal microbiota and elicited tissue inflammation (4, 5). Inflammatory cytokines regulate the innate immune responses shaped by the microbiota and affect the rate of intestinal epithelial cell proliferation (6–9). Among these cytokines are type I interferons (IFN) that activate a cognate cell surface receptor (consisting of the IFNAR1 and IFNAR2 chains) and signal to induce the transcription of IFN-stimulated genes (ISGs), some of which are known for their antiproliferative properties (10). Despite the known suppressive effects of IFN on cell proliferation and constitutive induction of IFN in the gut (11, 12), the role of these cytokines in regulating intestinal epithelium proliferation and function remains poorly understood.

Adequate expression of the IFNAR1 chain of the IFN receptor is required for all IFN effects (13–15). Genetic studies using the *Ifnar1* knockout in mice have yet to establish the role of IFN in regulating intestinal epithelial cell proliferation. Ablation of *Ifnar1*, specifically in IECs (*Ifnar1* <sup>$\Delta$ IEC</sup>), resulted in only a modest increase in bromodeoxyuridine (BrdU) labeling, and this increase was dependent on the changes in the commensal microbiota (16). However, neither alteration in the microbiome profile (17) nor increased IEC proliferation (17, 18) was observed in mice lacking *Ifnar1* in all tissues compared to wild-type mice. These data suggest either that IFN do not play an important role in regulating intestinal epithelium proliferation or that genetic differences between *Ifnar1*<sup>+/+</sup> and *Ifnar1*<sup>-/-</sup> animals are masked by additional factors.

Indeed, high levels of cell surface IFNAR1 are specifically required for the antiproliferative effects of IFN as opposed to their ability to elicit an antiviral state (14, 19). These levels of IFNAR1 are tightly regulated by its phosphorylation-dependent ubiquitination and subsequent endocytosis and lysosomal degradation (20–22). The rate-limiting event in these processes is the phosphorylation of serine residues within the IFNAR1 degnon that enables the recruitment of beta-transducin repeat containing protein ( $\beta$ Trcp) E3 ubiquitin ligase and IFNAR1 ubiquitination (21, 23). Importantly, while this phosphorylation can be induced by IFN via the activation of protein kinase D2 (24, 25), there is also a ligand-independent pathway that removes IFNAR1 from the surface of cells that are yet to encounter IFN (23, 26). This pathway was shown to be activated by inflammatory cytokines (27) and may contribute to the lack of phenotypic differences between wild-type and *Ifnar1* knockout mice under inflammatory conditions (28). We previously purified and characterized casein kinase 1 $\alpha$  (CK1 $\alpha$ ) as a major ligand-independent kinase that is capable of phosphorylating IFNAR1 *in vitro* (29).

Importantly, CK1 $\alpha$  is also a critical mediator of  $\beta$ -catenin ubiquitination and degradation (2). Priming phosphorylation of  $\beta$ -catenin by CK1 $\alpha$  greatly increases the phosphorylation of the  $\beta$ -catenin degnon by glycogen synthase kinase 3 $\beta$  (GSK3 $\beta$ ) (30,

Received 29 October 2015 Returned for modification 2 December 2015

Accepted 15 January 2016

Accepted manuscript posted online 25 January 2016

Citation Katlinskaya YV, Katlinski KV, Lasri A, Li N, Beiting DP, Durham AC, Yang T, Pikarsky E, Lengner CJ, Johnson FB, Ben-Neriah Y, Fuchs SY. 2016. Type I interferons control proliferation and function of the intestinal epithelium. *Mol Cell Biol* 36:1124–1135. doi:10.1128/MCB.00988-15.

Address correspondence to Serge Y. Fuchs, syfuchs@vet.upenn.edu.

Copyright © 2016, American Society for Microbiology. All Rights Reserved.

31) that is required for its recognition by the  $\beta$ Trcp E3 ubiquitin ligases and subsequent ubiquitination and proteasomal degradation (32–36). Our recent studies demonstrated that gut-specific knockout of the *Csnk1a1* gene that encodes CK1 $\alpha$  leads to robust stabilization of  $\beta$ -catenin and activation of Wnt target genes (37, 38). Intriguingly, ablation of *Csnk1a1* alone did not lead to either epithelial cell hyperproliferation or tumorigenesis. Instead, inactivation of CK1 $\alpha$  induced the DNA damage response (DDR) and p53/p21-dependent senescence. These events appear to prevent tumorigenesis driven by hyperactive  $\beta$ -catenin because the concurrent ablation of CK1 $\alpha$  with either p53 or p21 resulted in hyperproliferation and a rapid development of aggressive and invasive intestinal tumors (37, 38).

Here we determined the role of CK1 $\alpha$  in the regulation of IFNAR1 ubiquitination and levels *in vivo*. We found that despite the accumulation of IFNAR1 protein (but not mRNA), the ubiquitination of IFNAR1 was decreased in CK1 $\alpha$ -deficient intestinal tissues. In addition, the expression of IFN-stimulated genes was increased in the gut upon *Csnk1a1* ablation. As the lack of CK1 $\alpha$  stabilized both  $\beta$ -catenin and IFNAR1, the phenotype associated with the loss of *Csnk1a1* highlighted the contribution of IFN signaling to control IEC proliferation and function. Intriguingly, IFN signaling was required for the effective activation of p53 and p21 and induction of senescence and apoptosis in the CK1 $\alpha$ -deficient intestinal epithelium. Furthermore, the concurrent ablation of CK1 $\alpha$  with *Ifnar1* led to unrestricted IEC proliferation to an extent that caused profound aberrations of gut barrier function and rapid animal death. These results demonstrate that IFN play an important role in restricting intestinal epithelial cell proliferation elicited by the activated  $\beta$ -catenin pathway.

## MATERIALS AND METHODS

**Animals.** All experiments with animals were carried out under protocol 803995 approved by the IACUC of the University of Pennsylvania. All mice were on the C57BL/6 background, had water *ad libitum*, and were fed regular chow. *Ifnar1*<sup>-/-</sup> mice (a kind gift of Dong-Er Zhang, UCSD) were crossed with *Csnk1a1*<sup>lox/lox</sup> mice, which bear floxed *Csnk1a1* and *Vil1-Cre-ER*<sup>T2</sup> (37), to generate *Csnk1a1*<sup>lox/lox</sup>; *Ifnar1*<sup>+/+</sup> or *Csnk1a1*<sup>lox/lox</sup>; *Ifnar1*<sup>-/-</sup> mice bearing *Vil1-Cre-ER*<sup>T2</sup> (*Vil1-Cre-ER*<sup>T2</sup> in genotype identification is omitted for simplicity). Genotyping was performed on the tail of 4-week-old pups according to standard protocols using previously described primers (37).

Tamoxifen (Sigma) was dissolved in corn oil (Sigma), and mice were injected intraperitoneally (120 mg/kg of body weight) on two consecutive days. On day 5 after the last injection, mice were euthanized. The jejunum, the ileum, and the entire large intestine were flushed with ice-cold phosphate-buffered saline (PBS); cut open longitudinally; and subjected to fixation in 4% formaldehyde and paraffin embedding. Small pieces of the jejunum were embedded in Tissue-Tek OCT compound (Sakura) and frozen at -80°C. IECs were isolated from the middle part of the small intestine as described previously (39) but with the following slight modifications: intestinal cells were separated into single cells in Hanks' balanced salt solution containing 5 mM EDTA at 4°C for 30 min.

For antibiotic treatment, *Csnk1a1*<sup>Δgut</sup>; *Ifnar1*<sup>-/-</sup> mice were gavaged with 100 mg streptomycin (Sigma), and the drinking water was immediately replaced with filter-sterilized water containing ampicillin (1 g/liter; American Bioanalytical), vancomycin (0.5 g/liter; MP Biomedicals), neomycin (1 g/liter; Sigma), metronidazole (1 g/liter; Sigma), and 1% sucrose (Fisher). Antibiotic-containing water was replaced at least once a week during the course of the experiment. For all experimental groups, either mice were cohoused or their feces were swapped daily between cages to minimize potential differences in the gut microbiota.

**Histology and immunotechniques.** Sections (5  $\mu$ m) were cut for hematoxylin and eosin (H&E) staining and immunohistochemistry analysis. For immunohistochemistry, sections were incubated with antibodies to detect CK1 $\alpha$  (C-19 [1:1,000]; Santa Cruz Biotechnology),  $\beta$ -catenin (1:200; Cell Signaling), cyclin D1 (SP4 [1:100]; Thermo Scientific), Ki67 (2.5 mg/ml; BioLegend), cleaved caspase-3 (1:100; Cell Signaling Technology), and p53 (1:500; Novocasta). Secondary antibodies were horseradish peroxidase (HRP)-conjugated anti-rabbit, anti-goat, and anti-rat antibodies (Millipore, Cell Signaling Technology). 3,3'-Diaminobenzidine (DAB) chromogen (Lab Vision) was used for detection. For whole-tissue immunofluorescence, pieces of small intestine harvested from mice were frozen in Tissue-Tek OCT compound, cryosectioned by using Leica CM3050 S cryostats, fixed in acetone, washed, and blocked with PBS containing 5% goat serum. The sections were incubated for 1 h with primary antibodies to detect IFNAR1 (2  $\mu$ g/ml; Sino Biological),  $\gamma$ H2AX (1:100; Millipore), E-cadherin (1:500; Millipore), or TJP1/ZO-1 (1:100; Thermo Fisher). The sections were then washed, incubated with the corresponding secondary antibodies labeled with Alexa Fluor 488 or 594 (Invitrogen) for 1 h, washed again, and mounted onto coverslips by using mounting solution with 4',6-diamidino-2-phenylindole (DAPI) (Prolong Gold). For senescence-associated  $\beta$ -galactosidase (SA- $\beta$ Gal) staining (described in detail in reference 40), 10- $\mu$ m sections were cut from OCT-embedded frozen tissue and allowed to adhere to coated slides at 25°C for 1 min before fixation for 15 min. Staining was performed according to the instruction provided with the senescence  $\beta$ -galactosidase staining kit (catalog number 9860S; Cell Signaling). After staining, sections were counterstained with nuclear fast red, dehydrated, and mounted. Periodic acid-Schiff (PAS) staining for goblet cell determination was performed according to standard protocols. Numbers of  $\gamma$ H2AX-, IFNAR1-, and Ki67-positive foci per crypt/villus axis were determined by counting foci in 40 or 20 low-power fields (magnification of  $\times$ 200 or  $\times$ 400). The number of positive cells per crypt (Ki67, cleaved caspase-3, and SA- $\beta$ Gal) was determined by counting foci in 20 low-power fields (magnification of  $\times$ 200).

**Western blotting.** Proteins were extracted from intestinal epithelial cell pellets in protein lysis buffer containing protease and phosphatase inhibitors according to whole-cell extract protocols. IFNAR1 was immunoprecipitated from whole-cell lysates by using MAR1-5A3 (Leinco Technologies, Inc.), as previously described (28). Membranes were incubated with antibodies to detect IFNAR1 (2  $\mu$ g/ml; Sino Biological), ubiquitin (Ub) (P4D1 [1:1,000]; Santa Cruz Biotechnology), CK1 $\alpha$  (C-19 [1:1,000]; Santa Cruz Biotechnology), p21<sup>CIP1/WAF1</sup> (ab7960 [1:1,000]; Abcam), interferon regulatory factor 7 (IRF7) (ab62505 [1:1,000]; Abcam), ZO-1 (1:100; Thermo Fisher), and  $\beta$ -actin (AC-74 [1:5,000]; Sigma). Secondary antibodies conjugated to horseradish peroxidase were purchased from Millipore Bioscience Research Reagents. Blots were processed as previously described (23) and developed by using ECL (GE Healthcare).

**RNA analysis.** Total RNA was extracted from cell pellets by using TRIzol reagent and phenol-chloroform methods. RNA (1  $\mu$ g) was subjected to reverse transcription using a first-strand cDNA synthesis kit (Thermo Scientific), and mRNA expression levels were measured by quantitative real-time PCR using an Applied Biosystems 7500 Fast real-time PCR system. Relative quantities of gene transcripts were normalized to  $\beta$ -actin transcript levels. Sequences of PCR primers are as follows: 5'-TAGGCGGAATGAAGATGGAC (forward primer for *Axin2*), 5'-CTGGTCACCAACAAGGAGT (reverse primer for *Axin2*), 5'-CAGTATCTCCGGCTGAGG (forward primer for *Cd44*), 5'-GCCAACTTCATTGTGCCAT (reverse primer for *Cd44*), 5'-GGTGCAGGATCGGATCT (forward primer for *Csnk1a1*), 5'-TTCCTGACTGCTTCCTCGC (reverse primer for *Csnk1a1*), 5'-TTGACTGCCGAGAAGTTGTG (forward primer for *cyclin D1*), 5'-CCACTGAGCTTGTTACCA (reverse primer for *cyclin D1*), 5'-CTGCTGCCTGGGCTTCATAG (forward primer for *Ifitm3*), 5'-GGATGCTGAGGACCAAGGTG (reverse primer for *Ifitm3*), 5'-TCCACAGCATATCCAGACA (forward primer for *Cdkn1a*), 5'-AGACAACGGCACACTTTGCT (reverse primer for *Cdkn1a*), 5'-GGAGCTC

AGCAAGACTCTGG (forward primer for *Sox9*), 5'-TGTAATCGGGGTGGTCTTCT (reverse primer for *Sox9*), 5'-GCCTACTCGTCGGA GGAA (forward primer for *Ascl2*), 5'-CCAACTGGAAAAGTCAAGCA (reverse primer for *Ascl2*), 5'-CCCTGTGAAGGAAGTGGCTA (forward primer for *Oas2*), 5'-CTGTTGGAAGCAGTCCATGA (reverse primer for *Oas2*), 5'-GTCAGAGTGGAAATCCTAAG (forward primer for *Ifn $\beta$* ), 5'-ACAGCATCTGTGTTGAAG (reverse primer for *Ifn $\beta$* ); 5'-CGACCAAGTGTGAATCTCTTAC (forward primer for *Ifnar1*), 5'-ATCAACC TCATTCCACGAAGAT (reverse primer for *Ifnar1*), 5'-ACCCGAAACTGATGCTGTGGATAG (forward primer for *Tjp1*), 5'-AAATGGCCGGG CAGAGACTTGTGTA (reverse primer for *Tjp1*), 5'-TGAAACGCCGAC CTATCCTTA (forward primer for *Trp53*), 5'-GGCACAAACACGAACC TCAAA (reverse primer for *Trp53*), 5'-ATATTAACCGCGCTACGAC (forward primer for *Bak1*), 5'-AGCGCATCTTGGTGAAGAGT (reverse primer for *Bak1*), 5'-ATGCTGTGGATCTGGGCTGTCTCT (forward primer for *Fas*), 5'-GCATAATGGTCTTGTCCATG (reverse primer for *Fas*), 5'-CCTCAAGTTTTGCCCTTTA (forward primer for *Casp1*), 5'-CCTTCTTAATGCCATCATCTT (reverse primer for *Casp1*), 5'-AGAGG GAAATCGTGGCTGAC (forward primer for  $\beta$ -actin), and 5'-CAATAG TGATGACCTGGCCGT (reverse primer for  $\beta$ -actin).

**Isolation and culture of intestinal crypts.** Crypt culture was performed as previously described (41). After intestinal crypt isolation, a total of 500 crypts were mixed with 50  $\mu$ l of Matrigel (BD Biosciences) and plated into 24-well plates. After polymerization of Matrigel, 500  $\mu$ l of crypt culture medium (Advanced Dulbecco's modified Eagle's medium [DMEM]–F-12 medium containing 50 ng/ml epidermal growth factor [EGF] [Invitrogen], 1  $\mu$ g/ml R-spondin [Peprotech], and 100 ng/ml Noggin [Peprotech]) was added. Organoids were treated with 10  $\mu$ M the CK1 inhibitor D4476 (Sigma), 10  $\mu$ g/ml IFN- $\beta$  neutralizing antibody (Leinco Technologies), and the corresponding vehicle or isotype controls. After 4 days of culture at 37°C, the numbers of live organoids were quantified.

**Microarray.** Microarray analyses were performed with an Illumina whole-genome array. Total RNA was isolated from intestinal epithelial cells of *Csnk1a1 $\Delta$ gut*, *Ifnar1 $^{+/+}$*  (single knockout [SKO]) and *Csnk1a1 $\Delta$ gut*; *Ifnar1 $^{-/-}$*  (double knockout [DKO]) mice at day 5 after the last tamoxifen treatment by using a miRNeasy minikit (Qiagen). Biotin-labeled cRNA samples were prepared by using a TargetAmp-Nano labeling kit (Epicentre) as recommended by the manufacturer. Thereafter, 0.75  $\mu$ g cRNA was hybridized to Illumina Sentrix Mouse-6 v.1 BeadChips, which were scanned with an Illumina BeadStation 500 instrument (both from Applied Biosystems-Life Technologies, Inc.). Data were collected with Illumina BeadStudio 3.1.1.0 software, and statistical analyses were conducted with IlluminaGUI R-package 15,70.

**Intestinal permeability assay.** Barrier function was evaluated by measuring *in vivo* paracellular permeability to fluorescence-labeled dextran. Mice were fasted for 4.5 h and then gavaged fed fluorescein isothiocyanate (FITC)-labeled 4.4-kDa dextran (FD4; Sigma). Plasma was obtained 5 h after gavage administration by terminal cardiac puncture after CO<sub>2</sub> anesthesia. The plasma FD4 concentration was calculated by comparing samples with serial dilutions of known standards by using a Varioskan Flash fluorimeter (Thermo Scientific) with excitation at 485 nm and emission at 530 nm.

**Statistical analyses.** Data are presented as averages  $\pm$  standard errors of the means (SEM). Statistical analysis was performed by using Microsoft Excel. Statistical significance was calculated by using a two-tailed Student *t* test. A *P* value of <0.05 was considered significant.

**Microarray data accession number.** Raw data were deposited in the GEO database under accession number GSE76512.

## RESULTS

**Activation of IFN signaling in response to CK1 $\alpha$  ablation.** To determine the role of CK1 $\alpha$  in the regulation of IFNAR1 levels and signaling in the intestinal epithelium, we crossed *Csnk1a1 $^{fl/fl}$*  mice with animals expressing *Vill1-Cre-ER $^{T2}$*  (37). Both strains harbored a double-wild-type allele for *Ifnar1* (*Ifnar1 $^{+/+}$* ). Treat-

ment of the progeny from these crosses with tamoxifen resulted in mice lacking CK1 $\alpha$  exclusively in the intestinal epithelium (*Csnk1a1 $\Delta$ gut*; *Ifnar1 $^{+/+}$*  [SKO]). The decrease in CK1 $\alpha$  expression in the intestinal epithelium was monitored by assessing the levels of *Csnk1a1* mRNA (Fig. 1A) and protein (Fig. 1B and C). We next crossed these mice to mice lacking *Ifnar1* and observed a similar extent of CK1 $\alpha$  ablation in these DKO mice (Fig. 1A to C).

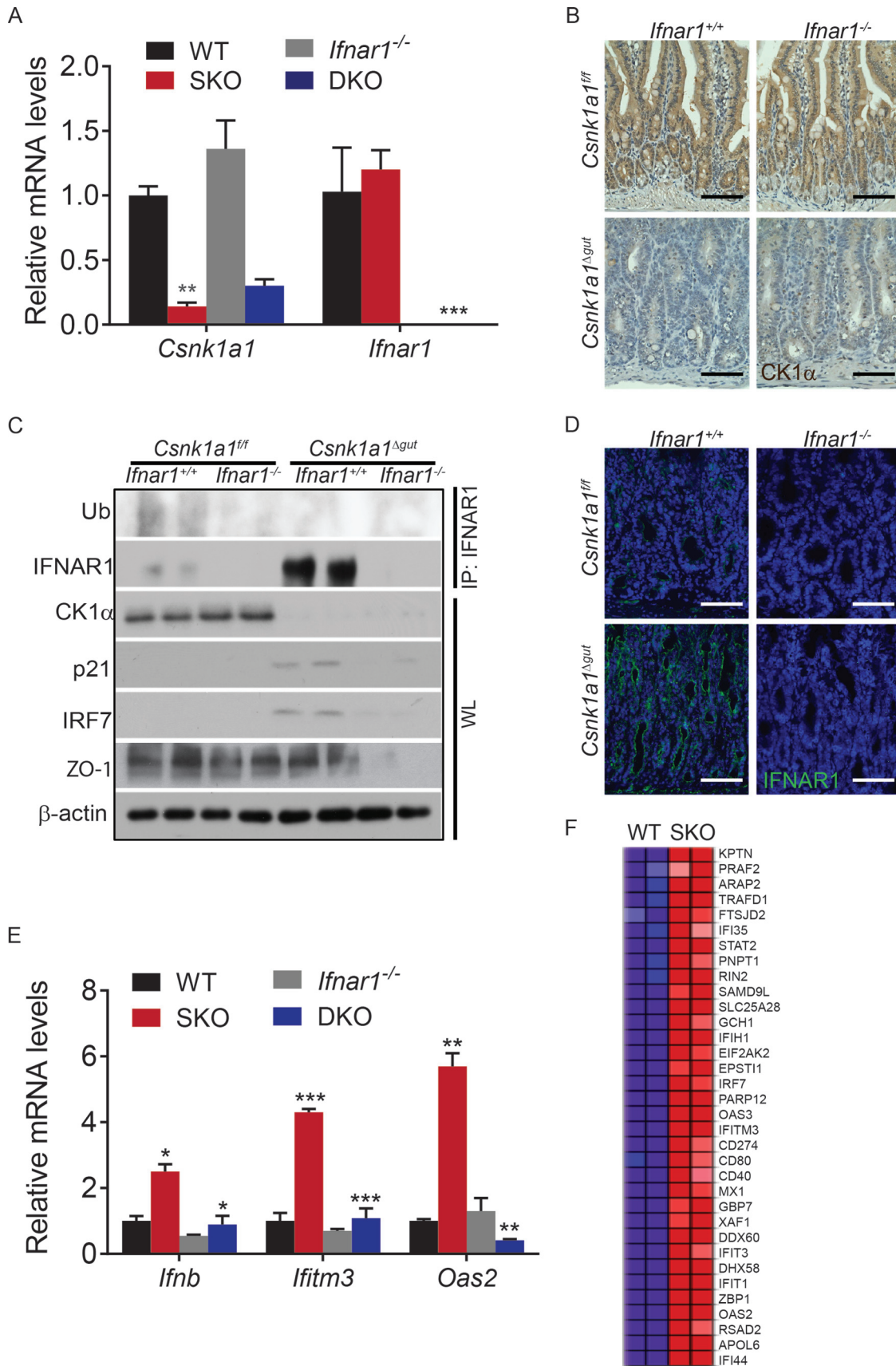
CK1 $\alpha$  can phosphorylate IFNAR1 within its degron *in vitro* (29). Phosphorylation of this degron enables ubiquitination of IFNAR1 (21, 22). Here we aimed to determine the role of CK1 $\alpha$  in the regulation of IFNAR1 ubiquitination and levels in the intestinal tissues. We detected IFNAR1 protein and its ubiquitination in intestinal epithelial tissue lysates from *Csnk1a1 $\Delta$ gut*; *Ifnar1 $^{+/+}$*  mice (Fig. 1C). Importantly, deletion of *Csnk1a1* resulted in decreased IFNAR1 ubiquitination concurrent with a dramatic increase in the overall level of IFNAR1 protein (Fig. 1C and D). Given that *Ifnar1* mRNA levels were not affected by the ablation of *Csnk1a1* (Fig. 1A), these data are consistent with the hypothesis that CK1 $\alpha$  is a major regulator of IFNAR1 ubiquitination and proteolytic degradation *in vivo*.

Importantly, the IFN-inducible IRF7 protein was upregulated in CK1 $\alpha$ -deficient mice (Fig. 1C). Furthermore, CK1 $\alpha$  ablation induced the mRNA levels of *Ifnb* along with a number of other IFN-stimulated genes (Fig. 1E and F). Induction of mRNA of the ligand IFN- $\beta$  and stimulation of *Oas2* and *Ifitm3* expression were likely dependent on intact IFN signaling because these increases were not seen in tissues from *Csnk1a1 $\Delta$ gut*; *Ifnar1 $^{-/-}$*  mice (Fig. 1E). Collectively, these data suggest that the ablation of CK1 $\alpha$  leads to the accumulation of IFNAR1, induction of IFN expression, and activation of expression of IFN-stimulated genes in the intestinal epithelium.

**Inhibition of IFN signaling attenuates DNA damage responses in CK1 $\alpha$ -deficient mouse intestines.** Our previous work demonstrated that ablation of CK1 $\alpha$  in the gut resulted in the stabilization and accumulation of  $\beta$ -catenin, activation of Wnt target genes, and induction of DDR signaling (37). Moreover, DNA damage was shown to both induce IFN production (42, 43) and be further stimulated by IFN signaling (44). Thus, we sought to investigate the role of IFN signaling in the DDR by comparing the consequences of CK1 $\alpha$  ablation in *Ifnar1 $^{+/+}$*  and *Ifnar1 $^{-/-}$*  mice.

Regardless of the status of *Ifnar1*, we observed that CK1 $\alpha$  deletion leads to a robust accumulation of  $\beta$ -catenin (Fig. 2A). Consistent with this result, similar levels of induction of cyclin D1 protein was observed in *Csnk1a1 $\Delta$ gut*; *Ifnar1 $^{+/+}$*  and *Csnk1a1 $\Delta$ gut*; *Ifnar1 $^{-/-}$*  mice (Fig. 2B). Furthermore, animals of both genotypes exhibited comparable increases in the levels of several Wnt target genes, including *Sox9*, *Ccnd1*, *Axin2*, *Ascl2*, and *Cd44* (Fig. 2C). These results indicate that IFN signaling is dispensable for  $\beta$ -catenin stabilization and transcriptional activation in the absence of CK1 $\alpha$ .

Intriguingly, the concurrent ablation of CK1 $\alpha$  and *Ifnar1* noticeably decreased the extent of DDR signaling as seen from the number of phosphorylated histone H2AX foci in CK1 $\alpha$ -deficient tissues (Fig. 3A and B). Our previously reported results showed that IFN- $\beta$  induced in response to DNA damage can further augment the extent of this damage. Furthermore, DDR-stimulated IFN was shown to play an important role in the induction of the p53 tumor suppressor protein transcriptional target gene *Cdkn1a*, which encodes the p21<sup>CIP1/WAF1</sup> protein (43). The accumulation



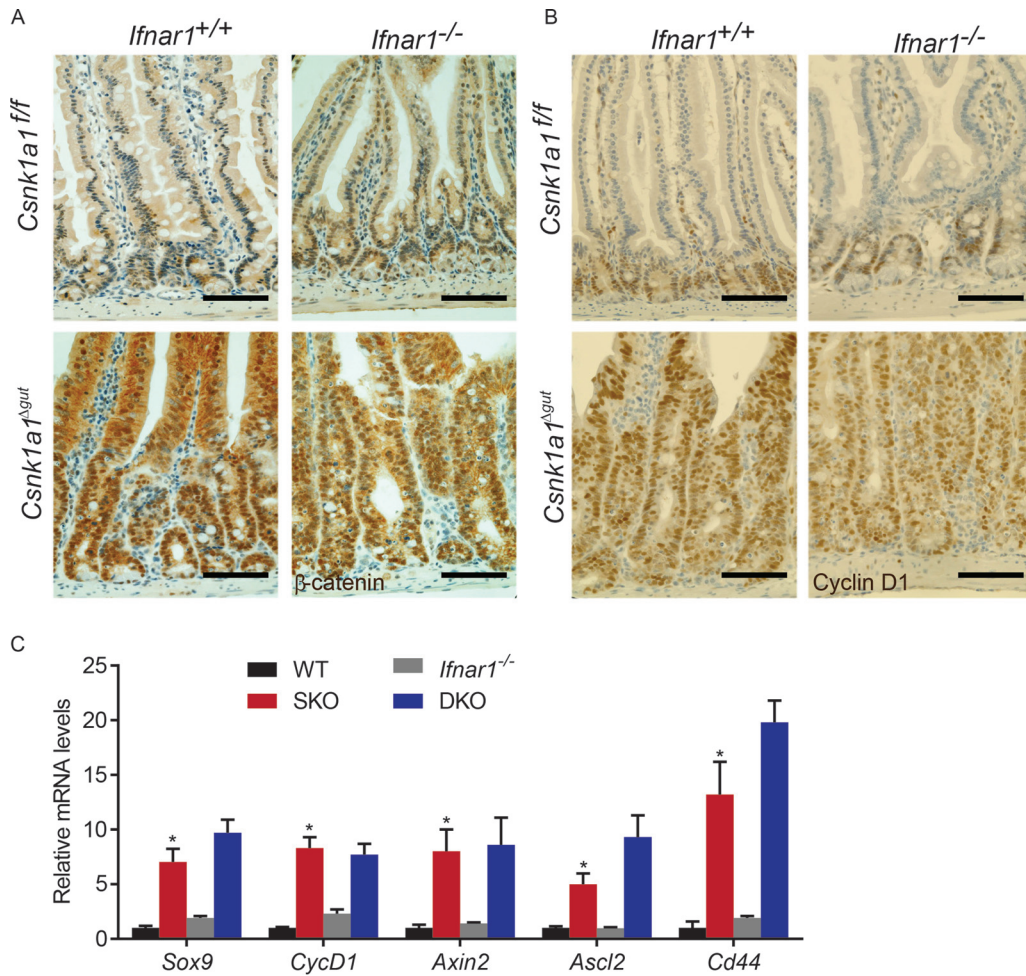


**FIG 2** Knockout of the gene encoding CK1 $\alpha$  induces  $\beta$ -catenin stabilization and Wnt hyperactivation in murine intestines from *Ifnar1*<sup>-/-</sup> mice. (A) Immunohistochemistry analysis of  $\beta$ -catenin expression in intestinal tissues from mice of the indicated genotypes. Bars, 100  $\mu$ m. (B) Immunohistochemistry analysis of cyclin D1 expression in intestinal tissues from mice of the indicated genotypes. Bars, 100  $\mu$ m. (C) Relative mRNA levels of the indicated Wnt target genes in intestinal epithelial cells from mice of the indicated genotypes as assessed by quantitative PCR (levels in untreated *Csnk1a1*<sup>lox/lox</sup>; *Ifnar1*<sup>+/+</sup> mice are taken as 1.0). Data are shown as averages  $\pm$  SEM; an asterisk above *Csnk1a1* <sup>$\Delta$ gut</sup> (SKO) indicates a significant difference between wild-type (WT) and SKO mice. \*,  $P < 0.05$ .

of p53 protein seen upon the deletion of *Csnk1a1* was not affected by the status of *Ifnar1* (Fig. 3C). However, inactivation of *Ifnar1* led to noticeable decreases in the levels of p21<sup>CIP1/WAF1</sup> protein (Fig. 1C) and mRNA (Fig. 3D) in CK1 $\alpha$ -deficient tissues. Given that *Ifnar1* ablation also attenuated the induction of other p53-dependent genes (Fig. 3D and E), these results strongly suggest an important role for IFN signaling in the activation of DDR and p53 activities in CK1 $\alpha$ -deficient intestinal tissues.

**Endogenous IFN restrict proliferation of intestinal epithelial cells and elicit their apoptosis.** We previously postulated that *Csnk1a1* ablation simultaneously elicits the proproliferative activity of canonical Wnt pathway target genes through  $\beta$ -catenin stabilization along with another yet-to-be-understood antiproliferative pathway that activates p53-p21, restricts IEC proliferation, and prevents tumorigenesis in spite of constitutive  $\beta$ -catenin activity (37). We therefore investigated the role of IFN in inhibiting

**FIG 1** Activation of IFN signaling in response to CK1 $\alpha$  ablation. (A) Relative levels of *Csnk1a1* and *Ifnar1* mRNAs in intestinal tissues from mice of the indicated genotypes. Levels of mRNA in intestinal tissues from untreated *Csnk1a1*<sup>lox/lox</sup>; *Ifnar1*<sup>+/+</sup> mice were taken as 1.0. Data are shown as averages  $\pm$  SEM; asterisks above *Csnk1a1* <sup>$\Delta$ gut</sup> (SKO) indicate a significant difference between wild-type (WT) and SKO mice, and asterisks above *Csnk1a1* <sup>$\Delta$ gut</sup>; *Ifnar1*<sup>-/-</sup> (DKO) indicate a significant difference between SKO and DKO mice. \*,  $P < 0.05$ ; \*\*,  $P < 0.01$ ; \*\*\*,  $P < 0.001$ . (B) Immunohistochemistry analysis of CK1 $\alpha$  levels in intestinal tissues from mice of the indicated genotypes. For all immunohistochemistry, brown indicates specific immunostaining and purple indicates nuclear hematoxylin staining. Bars, 100  $\mu$ m. (C) Western blotting of intestinal epithelial cells from mice of the indicated genotypes. IRF7 protein levels serve as an IFN-induced gene product control. Levels of  $\beta$ -actin were used as a loading control. (D) Immunofluorescence analysis of IFNAR1 expression in intestinal tissues from mice of the indicated genotypes. Bars, 100  $\mu$ m. (E) Relative mRNA levels of the indicated IFN-stimulated genes in IECs from mice of the indicated genotypes assessed by quantitative PCR (levels in untreated *Csnk1a1*<sup>lox/lox</sup>; *Ifnar1*<sup>+/+</sup> mice are taken as 1.0). (F) Heat map showing upregulation of IFN-induced genes in *Csnk1a1* <sup>$\Delta$ gut</sup> (wild-type) versus *Csnk1a1* <sup>$\Delta$ gut</sup> (SKO) IECs at day 5 after CK1 $\alpha$  ablation. Total RNA samples from three mice per genotype were pooled for analysis. The IFN gene signature is the Bosco interferon-induced antiviral module.

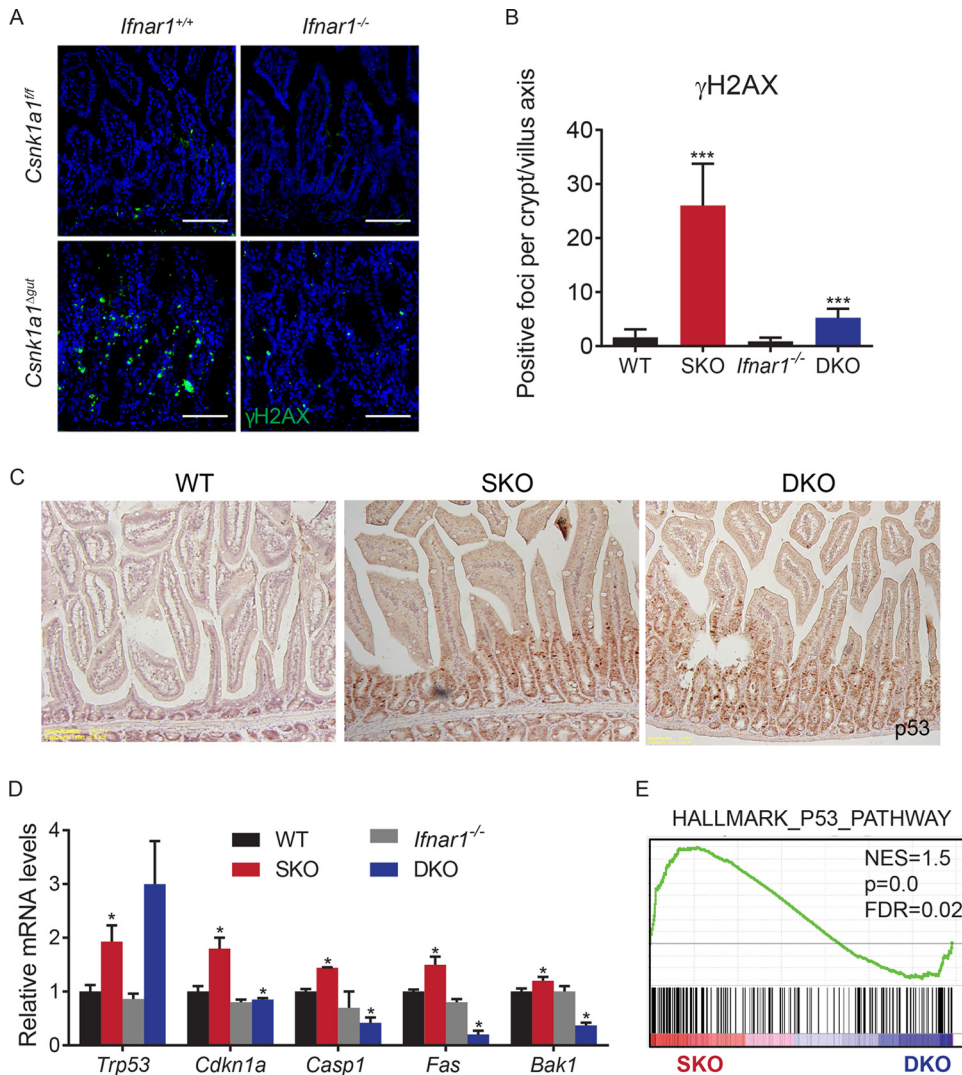


**FIG 3** Inhibition of IFN signaling suppresses DNA damage responses in CK1 $\alpha$ -deficient mouse intestines. (A) Immunofluorescence analysis of  $\gamma$ H2AX expression in intestinal tissues from mice of the indicated genotypes. Bar, 100  $\mu$ m. (B) Quantitation of the number of  $\gamma$ H2AX-positive foci per basal crypt in small intestines of three mice (30 to 50 crypts/villi were analyzed for each mouse). Data are shown as averages  $\pm$  SEM; asterisks above *Csnk1a1* <sup>$\Delta$ gut</sup> (SKO) indicate a significant difference between wild-type (WT) and SKO mice, and asterisks above *Csnk1a1* <sup>$\Delta$ gut</sup>; *Ifnar1*<sup>-/-</sup> (DKO) indicate a significant difference between SKO and DKO mice. \*,  $P < 0.05$ ; \*\*\*,  $P < 0.001$ . (C) Immunohistochemical analysis of p53 levels in intestinal tissues from mice of the indicated genotypes. Magnification,  $\times 10$ . (D) Relative mRNA levels of the indicated p53 target genes in IECs from mice of the indicated genotypes as assessed by quantitative PCR (levels in untreated *Csnk1a1*<sup>lox/lox</sup>; *Ifnar1*<sup>+/+</sup> mice are taken as 1.0). (E) GSEA of the transcriptome profiles showing a significant enrichment of p53 target gene signatures in *Csnk1a1* <sup>$\Delta$ gut</sup> (SKO) versus *Csnk1a1* <sup>$\Delta$ gut</sup>; *Ifnar1*<sup>-/-</sup> (DKO) IECs at day 5 after CK1 $\alpha$  ablation. NES, normalized enrichment score; FDR, false discovery rate.

epithelial cell proliferation. Intriguingly, immunofluorescence staining demonstrates the mutual exclusion of the IFNAR1 protein with the marker of cell replication Ki67 in normal intestine (Fig. 4A and B). Whereas Ki67 staining in *Ifnar1*<sup>+/+</sup> mice was elevated upon *Csnk1a1* ablation, a further significant increase was seen in DKO mice (Fig. 4C and D). Consistent with this finding, the number of senescence-associated  $\beta$ -galactosidase (SA- $\beta$ gal)-positive cells was also dramatically lower in intestinal tissues of *Csnk1a1* <sup>$\Delta$ gut</sup>; *Ifnar1*<sup>-/-</sup> double-knockout mice (Fig. 4E and F). Finally, gene set enrichment analysis (GSEA) revealed a significant increase in the expression of genes associated with cell proliferation in *Csnk1a1* <sup>$\Delta$ gut</sup>; *Ifnar1*<sup>-/-</sup> double-knockout mice versus mice with the *Csnk1a1* <sup>$\Delta$ gut</sup> knockout alone (Fig. 4G). Collectively, these

results indicate that IFN signaling plays an important role in restricting IEC proliferation within the context of  $\beta$ -catenin stabilization caused by the inactivation of CK1 $\alpha$ .

Persistent activation of the Wnt pathway by stabilized  $\beta$ -catenin was shown to increase the number of apoptotic cells in the intestine (37, 45). Importantly, the concurrent deletion of *Ifnar1* and *Csnk1a1* decreased the enrichment of the apoptosis-associated gene signature (Fig. 4H) and decreased the number of cleaved caspase-3-positive cells (Fig. 4I and J). Taken together with the lower level of induction of p53-dependent proapoptotic genes such as *Casp1*, *Fas*, and *Bak1* (Fig. 3D), these results implicate IFN signaling in apoptosis that occurs upon constitutive  $\beta$ -catenin stabilization.

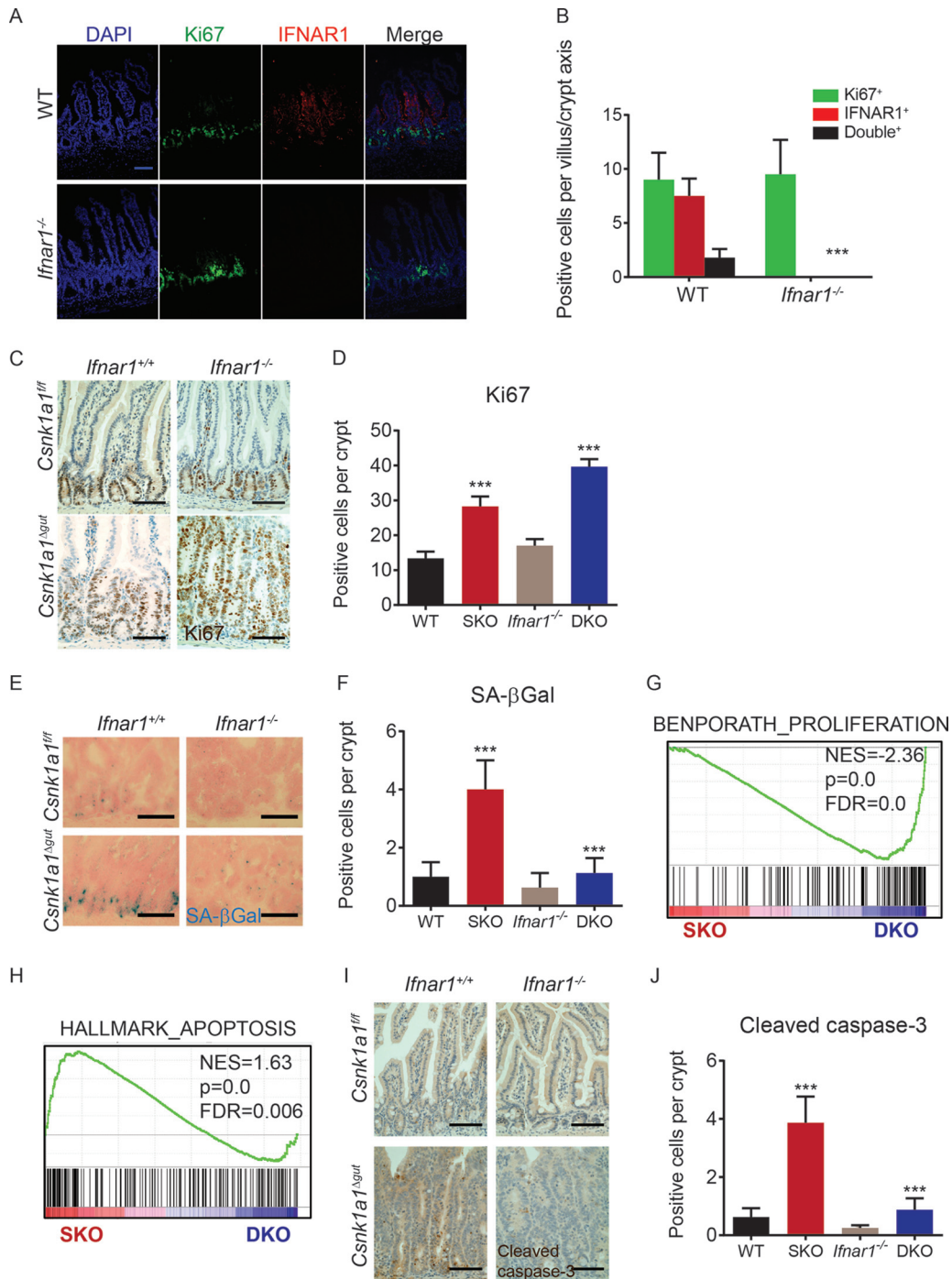


**FIG 4** Endogenous IFN restrict proliferation of intestinal epithelial cells and elicit their apoptosis. (A) Double-immunofluorescence analysis of IFNAR1 and Ki67 expression in intestinal tissues from mice of the indicated genotypes. Bar, 100  $\mu$ m. (B) Quantitation of the number of IFNAR1-positive, Ki67-positive, or double-positive cells per crypt/villus axis in the small intestines of three mice (30 to 50 crypts/villi were analyzed for each mouse). Data are shown as averages  $\pm$  SEM; asterisks above *Csnk1a1* <sup>$\Delta$ gut</sup> (SKO) indicate a significant difference between wild-type (WT) and SKO mice, and asterisks above *Csnk1a1* <sup>$\Delta$ gut</sup>; *lfnar1*<sup>-/-</sup> (DKO) indicate a significant difference between SKO and DKO mice. \*\*\*,  $P < 0.001$ . (C) Immunohistochemistry analysis of Ki67 levels in intestinal tissues from mice of the indicated genotypes. Bars, 100  $\mu$ m. (D) Quantitation of the number of Ki67-positive cells per basal crypt in the small intestines of three mice (30 to 50 crypts were analyzed for each mouse). \*\*\*,  $P < 0.001$  for differences between SKO and WT and between SKO and DKO mice. (E) Analysis of SA- $\beta$ Gal-positive cells in intestinal tissues (counterstained with nuclear fast red) from mice of the indicated genotypes. (F) Quantitation of the number of SA- $\beta$ Gal-positive cells per basal crypt in the small intestines of three mice (30 to 50 crypts were analyzed for each mouse). (G) GSEA of transcriptome profiles showing a significant enrichment of proliferation-associated gene signatures in *Csnk1a1* <sup>$\Delta$ gut</sup>; *lfnar1*<sup>-/-</sup> (DKO) versus *Csnk1a1* <sup>$\Delta$ gut</sup> (SKO) intestinal epithelial cells at day 5 after CK1 $\alpha$  ablation. NES, normalized enrichment score; FDR, false discovery rate. (H) GSEA of transcriptome profiles showing a significant enrichment of apoptosis-associated gene signatures in *Csnk1a1* <sup>$\Delta$ gut</sup> (SKO) versus *Csnk1a1* <sup>$\Delta$ gut</sup>; *lfnar1*<sup>-/-</sup> (DKO) IECs at day 5 after CK1 $\alpha$  ablation. (I) Immunohistochemistry analysis of cleaved caspase-3 levels in intestinal tissues from mice of the indicated genotypes. (J) Quantitation of the numbers of cleaved caspase-3-positive cells per basal crypt in the small intestines of three mice (30 to 50 crypts were analyzed for each mouse).

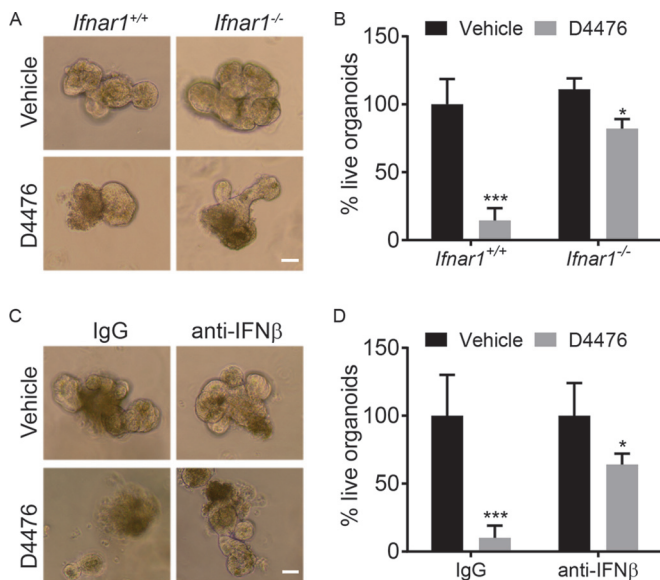


**FIG 5** Alterations in CK1 $\alpha$  and IFNAR1 levels affect intestinal organoid growth and survival. (A) Representative bright-field images of wild-type (WT) and *Ifnar1*<sup>-/-</sup> intestinal organoids treated with 10  $\mu$ M the CK1 $\alpha$  inhibitor D4476 at day 4. (B) Quantitation of live organoids in wild-type and *Ifnar1*<sup>-/-</sup> cultures compared with their vehicle-treated counterparts at day 4 (at least 10 random fields were analyzed for each culture). Data are shown as averages  $\pm$  SEM. \*,  $P < 0.05$ ; \*\*\*,  $P < 0.001$ . (C) Representative bright-field images of WT organoids treated with 10  $\mu$ M the CK1 $\alpha$  inhibitor D4476 in the presence or absence of 10  $\mu$ g/ml IFN- $\beta$  neutralizing antibodies at day 4. (D) Quantitation of live organoids in WT cultures compared with vehicle- and IgG-treated counterparts at day 4 (at least 10 random fields were analyzed for each culture).

Alterations in CK1 $\alpha$  and IFNAR1 levels can affect intestinal cell growth and survival directly or/and indirectly. To assess the direct contribution of these regulators, we assessed the proliferation and viability of IECs grown *ex vivo* as organoid cultures. Treatment of mouse intestinal crypt cultures with the CK1 inhibitor D4476 resulted in decreased overall organoid size and viability (Fig. 5). Importantly, organoids from *Ifnar1* knockout mice were less sensitive to the effects of D4476 (Fig. 5A and B). Furthermore, the inhibition of organoid growth by D4476 was noticeably attenuated by the addition of neutralizing antibodies against mouse IFN- $\beta$  (Fig. 5C and D). These results suggest that IFN mediate cell-autonomous growth restriction upon CK1 inactivation.

#### CK1 $\alpha$ and IFN pathways regulate intestinal barrier function.

Loss of the tumor suppressor and  $\beta$ -catenin destruction complex component *Apc* in the small and large intestines leads to dramatic increases in proliferation, loss of differentiated goblet cells, and rapid animal death, probably due to an inability to absorb water and electrolytes (46). While the inactivation of both CK1 $\alpha$  and adenomatous polyposis coli (APC) in the gut led to the stabilization of  $\beta$ -catenin and activation of the Wnt-inducible genes, a markedly different gene expression profile was seen in *Csnk1a1* <sup>$\Delta$ gut</sup>; *Ifnar1*<sup>+/+</sup> mice (37) and in *Apc* <sup>$\Delta$ gut</sup>; *Ifnar1*<sup>+/+</sup> mice (46). Intriguingly, a significant enrichment for the genes altered in the latter mice was seen upon the concurrent ablation of CK1 $\alpha$  and IFNAR1 (Fig. 6A). The mild hyperplasia of the small intestine (Fig. 6B) and colonic epithelium (Fig. 6C) as well as the progressive loss of goblet cells (Fig. 6D and E) observed in *Csnk1a1* <sup>$\Delta$ gut</sup>; *Ifnar1*<sup>-/-</sup> mice were indeed somewhat reminiscent of the phenotype in *Apc* <sup>$\Delta$ gut</sup>; *Ifnar1*<sup>+/+</sup> animals.

Furthermore, *Csnk1a1* <sup>$\Delta$ gut</sup>; *Ifnar1*<sup>-/-</sup> mice rapidly became moribund within a week after tamoxifen treatment was completed (Fig. 7A). Their life span could be extended by intraperitoneal injections of buffered saline solution, suggesting that an imbalance of water and electrolytes due to a differentiation block and potential loss of barrier function contributed to this early lethality. To test barrier function, we administered fluorescent dextran by gavage into the gastrointestinal tract of *Csnk1a1*/*Ifnar1*-deficient and control animals. *Csnk1a1* <sup>$\Delta$ gut</sup>; *Ifnar1*<sup>-/-</sup> double-knockout mice exhibited markedly increased translocation of dextran into the bloodstream, consistent with compromised barrier function (Fig. 7B). While the levels of E-cadherin in *Csnk1a1* <sup>$\Delta$ gut</sup> mice were not affected by the status of *Ifnar1*, the double-knockout mice displayed decreased levels of the ZO-1 tight junction protein (Fig. 1C and 7C) and its mRNA (Fig. 7D). These results implicate the IFN pathway in regulating the barrier function of the gut.

Importantly, *Csnk1a1*/*Ifnar1*-deficient mice eventually became moribund despite the administration of buffered saline solution (Fig. 7A), suggesting additional mechanisms by which the IFN pathway contributes to intestinal homeostasis. A number of studies suggested an important role of microbiota in IFN induction and effects of IFN on innate immunity responses to commensal bacteria (reviewed in reference 47). Consistent with this role of IFN, the stromal elements of the gut in *Csnk1a1* <sup>$\Delta$ gut</sup>; *Ifnar1*<sup>-/-</sup> mice displayed signs of injury and leukocyte infiltration and contained enlarged and inflamed lymph nodes. A robust inflammatory response was seen near the basement membrane, including leukocyte infiltration, combined with mucosal injury and increased epithelium permeability (Fig. 7E). Observed alterations were indicative of an increased microbiota-induced ability to penetrate the barrier and induce inflammation. Indeed, treatment of *Csnk1a1*/*Ifnar1*-deficient mice with antibiotics efficiently prevented their death (Fig. 7A). These data collectively suggest that IFN signaling plays an important role in maintaining intestinal barrier functions and homeostasis of the host interaction with the microbiota.

#### DISCUSSION

Our data presented here demonstrate that induction of IFN signaling appears to contribute to the activation of the DNA damage responses and apoptotic pathways as well as the suppression of intestinal epithelium proliferation that occurs upon the inactivation of CK1 $\alpha$ . The latter event stabilizes both  $\beta$ -catenin and IFNAR1, thereby highlighting the conditions that determine the role of IFN signaling in restricting IEC proliferation. In addition, IFN contributes to the vitally important function of maintenance of intestinal barrier function.

CK1 $\alpha$  is capable of phosphorylating numerous proteins and affecting a multitude of signaling pathways and transcriptional activities toward specific genes (reviewed in reference 48). Whereas CK1 $\alpha$  was capable of phosphorylating the IFNAR1 degen *in vitro* (29), the role of other kinases in stimulating the recruitment of  $\beta$ Tcrp to IFNAR1 and promoting its ubiquitination, endocytosis, and degradation was also demonstrated (24, 25). Our current data clearly characterize CK1 $\alpha$  as a major regulator of IFNAR1 ubiquitination and stability *in vivo* (Fig. 1). Furthermore, these results implicate this kinase in the negative regulation of the IFN pathway in intestinal tissues and underscore the importance of CK1 $\alpha$  function for the proliferation of the intestinal epithelium and its permeability.

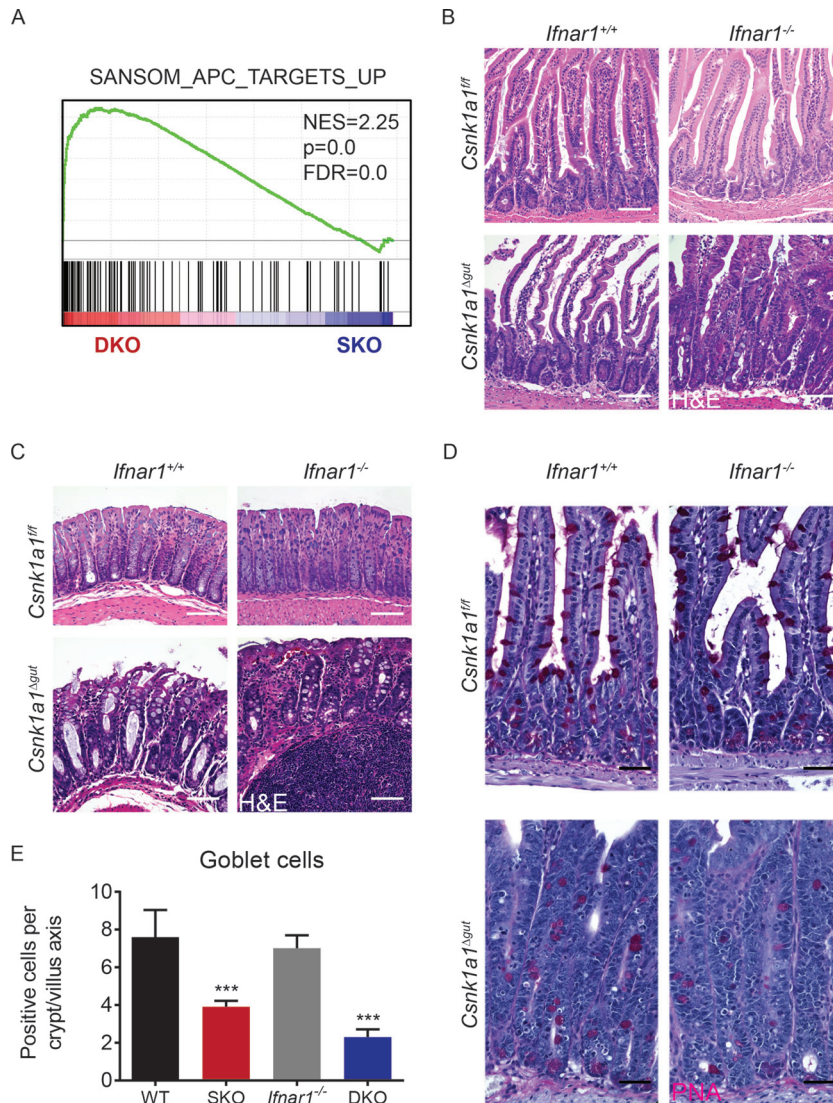


**FIG 6** Inhibition of IFN signaling increases proliferation and decreases numbers of goblet cells in intestinal tissues from *Csnk1a1*-deleted mice. (A) GSEA of transcriptome profiles showing a significant enrichment of genes upregulated upon APC deletion in *Csnk1a1*<sup>Δgut</sup>; *Ifnar1*<sup>-/-</sup> (DKO) versus *Csnk1a1*<sup>Δgut</sup> (SKO) intestinal epithelial cells at day 5 after CK1α ablation. NES, normalized enrichment score; FDR, false discovery rate. (B) H&E staining of small intestinal tissues from mice of the indicated genotypes. Bars, 100 μm. (C) H&E staining of colonic tissues from mice of the indicated genotypes. Bars, 100 μm. (D) PAS staining of small intestinal tissues from mice of the indicated genotypes. (E) Quantitation of the number of PAS-positive goblet cells per crypt/villus axis in the small intestines of three mice (30 to 50 crypts/villi were analyzed for each mouse). Data are shown as averages ± SEM; asterisks above SKO indicate a significant difference between wild-type (WT) and SKO mice, and asterisks above DKO indicate a significant difference between SKO and DKO mice. \*\*\*,  $P < 0.001$ .

Furthermore, our data suggest that the role of CK1α in regulating intestinal homeostasis is at least in part mediated by its effects on the stability and levels of IFNAR1 and the ensuing alterations in IFN signaling. Although microbiota-supported constitutive tonic IFN signaling has been described in the gut (11, 12), the role of this signaling in regulating gut renewal and function was a challenge to evaluate due to the potential phenotypic similarity of mice lacking the *Ifnar1* gene and wild-type mice exhibiting rapid IFNAR1 degradation under inflammatory conditions (28). The concurrent stabilization of IFNAR1 and β-catenin upon CK1α inactivation enabled us to determine that IFN plays an important role in restricting the proliferation and viability of the intestinal epithelium (Fig. 4 and 5) and contributes to the maintenance of the equilibrium of the host-microbiota interaction and barrier function (Fig. 7).

Our data further indicate that the IFN pathway contributes to the expression of p53-driven genes (including proapoptotic genes and *Cdkn1a*) stimulated in the absence of CK1α (Fig. 3). These data are consistent with our recently reported data demonstrating that IFN can amplify DNA damage responses (43) as well as with data from previous reports that exogenous IFN can trigger an increase in p53 activities (44, 49). Importantly, these effects of IFN may provide an additional mechanism for the activation of the p53 pathway in the CK1α-deficient gut in addition to the previously reported downregulation of MDMX and the ensuing stabilization of the p53 protein (37).

Intriguingly, activation of the p53 pathway was not observed in the *Apc*-deficient gut (37, 46). Given that the ablation of either CK1α or APC results in the stabilization of β-catenin and stimulation of the Wnt pathway, the difference between these pheno-

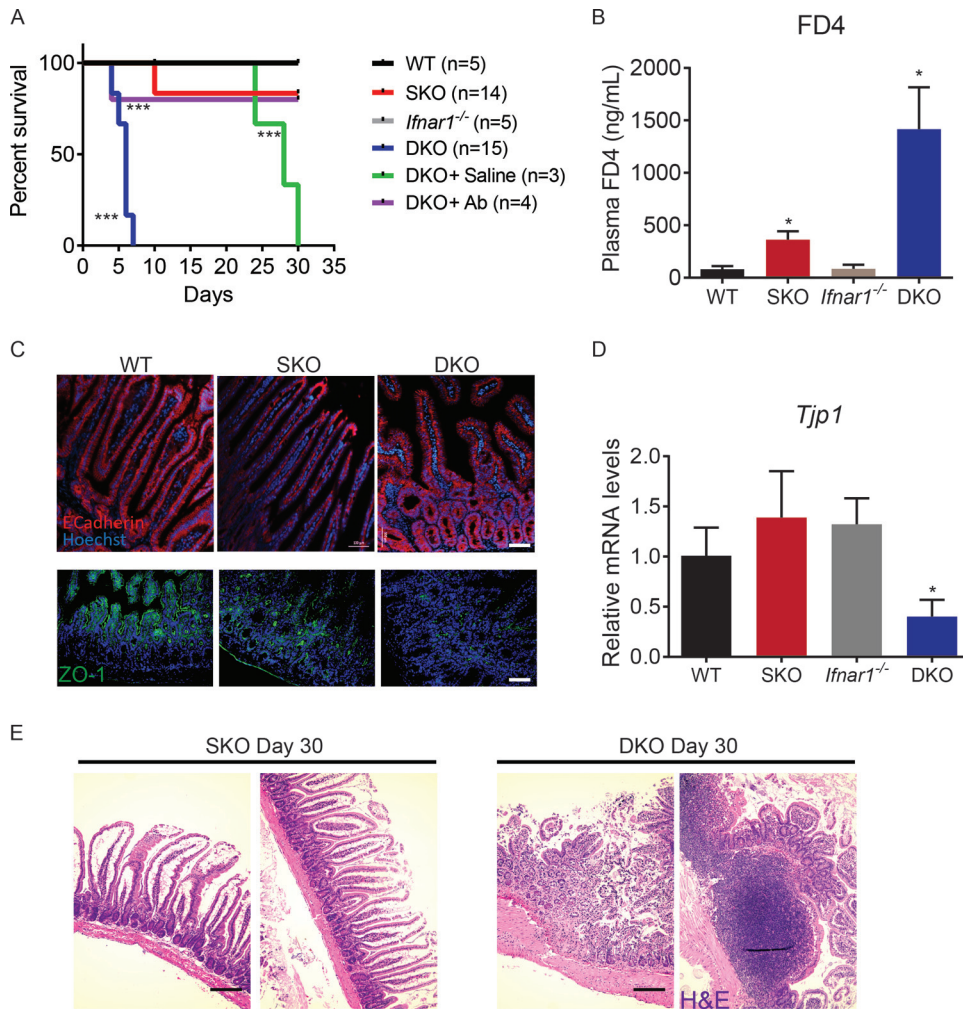


**FIG 7** CK1 $\alpha$  and IFN pathways regulate intestinal barrier function. (A) Kaplan-Meier survival analysis of mice of the indicated genotypes after induction of intestinal CK1 $\alpha$  ablation. *Csnk1a1* <sup>$\Delta$ gwt</sup>; *Ifnar1*<sup>-/-</sup> mice received intraperitoneal injections of 1 ml saline every day starting on day 1 after intestinal CK1 $\alpha$  ablation (DKO+Saline) or were administered antibiotics (Ab) in drinking water. \*\*\*,  $P < 0.001$ . Asterisks next to the DKO line indicate comparisons between SKO and DKO mice, asterisks next to the DKO+Saline indicate comparisons between DKO and DKO+Saline mice, and asterisks next to the DKO+Ab line indicate comparisons between DKO and DKO+Ab mice. Neither wild-type nor *Ifnar1*<sup>-/-</sup> mice died during the course of the experiment. (B) Levels of FITC-dextran (FD4) in plasma samples from mice of the indicated genotypes 5 h after FD4 gavage ( $n > 3$  for each group). Data are shown as averages  $\pm$  SEM; an asterisk above *Csnk1a1* <sup>$\Delta$ gwt</sup> (SKO) indicates a significant difference between wild-type (WT) and SKO mice, and an asterisk above *Csnk1a1* <sup>$\Delta$ gwt</sup>; *Ifnar1*<sup>-/-</sup> (DKO) indicates a significant difference between SKO and DKO mice. \*,  $P < 0.05$ . (C) Immunofluorescence analysis of E-cadherin (top) and tight junction protein 1 (TJP1) (zona occludens 1 [ZO-1]) (bottom) expression in intestinal tissues from mice of the indicated genotypes. Bar, 100  $\mu$ m. (D) Relative mRNA levels of *Tjp1* in intestinal epithelial cells from mice of the indicated genotypes as assessed by quantitative PCR (levels in untreated *Csnk1a1*<sup>lox/lox</sup>; *Ifnar1*<sup>+/+</sup> mice are taken as 1.0). (E) H&E staining of intestinal tissues from mice of the indicated genotypes at day 30 after tamoxifen treatment (DKO mice were treated with saline). Bar, 200  $\mu$ m.

types and underlying gene profile signatures can be explained by at least two diverse reasons. First, APC possesses important functions that do not depend on the timely degradation of  $\beta$ -catenin. For example, APC can bind RNA and regulate the microtubule scaffold (50). Furthermore, the loss of *Apc* leads to the upregulation of Musashi proteins, which are pleiotropic translational regulators that affect numerous important signaling cascades, including the mTorc1 pathway (51, 52). Second, characteristic for the deletion of *Csnk1a1* (but not *Apc*) induction of the DNA damage response, activation of the p53-driven genes, and cell senescence are likely augmented by IFN signaling activated by CK1 $\alpha$  deletion. Indeed, massive hyperproliferation of the intestinal epithelium leading to a defective barrier function and rapid animal death that was seen in *Csnk1a1/Ifnar1*-deficient mice is reminis-

cent of the phenotype observed upon intestinal deletion of APC (46) and is characterized by a similar gene expression signature (Fig. 6).

The restriction of proliferation of *Csnk1a1*-deficient IECs could be lifted by the concurrent inactivation of either p53, p21<sup>CIP1/WAF1</sup> (37, 38), or, to a lesser extent, IFNAR1 (this work). Importantly, ablation of either p53 or p21<sup>CIP1/WAF1</sup> in CK1 $\alpha$ -deficient animals led to the development of malignant tumors (37, 38). However, we did not observe these tumors in any groups of CK1 $\alpha$ /IFNAR1-deficient mice that developed a lethal disruption of intestinal barrier function (Fig. 7), suggesting a contribution of IFN-independent pathways to p53 function as a tumor suppressor in CK1 $\alpha$ -null intestines.

A few overlapping and non-mutually exclusive mechanisms by

which IFN contributes to the maintenance of the barrier function of the gut can be proposed. First, IFN-mediated restriction of the rate of cell proliferation should enable better differentiation, maturation, and establishment of the cohesive sheet of enterocytes and colonocytes. Second, IFN can contribute to immune defenses against conditionally pathogenic microbiota and intestinal inflammation. Katakura and coauthors previously reported a greater sensitivity of *Ifnar1*-null mice to intestinal inflammation caused by dextran sodium sulfate (53). Those authors also mentioned a positive effect of IFN on the protection of barrier properties of the epithelial cell sheet *in vitro*. Importantly, our results implicate IFN in regulating the expression of the ZO-1 protein involved in the formation of tight junctions that separate the basolateral epithelial space from the microbiota. Potential immune-related effects of IFN on the ability to withstand the pathogenic effects of microbiota are illustrated by the rescue of *Cnsk1a1/Ifnar1*-deficient mice upon administration of antibiotics (Fig. 7).

Genetic alterations in the IFNAR1 gene in humans were linked with the susceptibility locus for inflammatory bowel disease (54), and IFN-based pharmaceutical formulations have been used to treat patients with these disorders albeit with variable results (reviewed in reference 55). As evident from the literature and our current results, the effects of IFN on intestinal homeostasis are pleiotropic. Roles of IFN in antigen recognition and immune function, cell differentiation and proliferation, and gut barrier function are likely to contribute to the complexity of patient responses to IFN. Although some of the long-term IFN effects, such as suppression of tissue-regenerative abilities in the gastrointestinal tract, could be genuinely detrimental (17, 28), it is also plausible that rapid degradation of IFNAR1 may constitute an additional challenge for the efficacy of IFN-based therapies (reviewed in reference 13). Thus, future studies may determine the potential application of poorly bioavailable gut-restricted CK1 $\alpha$  inhibitors to stabilize IFNAR1 and improve intestinal barrier function.

## ACKNOWLEDGMENTS

We declare no conflict of interest.

This work was supported by NIH/NCI grants RO1 CA092900 and PO1 CA165997 (to S.Y.F.), including help from the Scientific Cell/Tissue Morphology Core and its principal investigator, Qian-Chun Yu.

We thank D. E. Zhang for reagents and A. Ortiz for help with manuscript preparation.

## FUNDING INFORMATION

Office of Extramural Research, National Institutes of Health (OER) provided funding to Serge Y. Fuchs under grant number CA165997. Office of Extramural Research, National Institutes of Health (OER) provided funding to Serge Y. Fuchs under grant number CA092900.

## REFERENCES

1. Heath JP. 1996. Epithelial cell migration in the intestine. *Cell Biol Int* 20:139–146. <http://dx.doi.org/10.1006/cbir.1996.0018>.
2. Clevers H. 2006. Wnt/beta-catenin signaling in development and disease. *Cell* 127:469–480. <http://dx.doi.org/10.1016/j.cell.2006.10.018>.
3. Pinto D, Clevers H. 2005. Wnt control of stem cells and differentiation in the intestinal epithelium. *Exp Cell Res* 306:357–363. <http://dx.doi.org/10.1016/j.yexcr.2005.02.022>.
4. Grivninkov SI, Greten FR, Karin M. 2010. Immunity, inflammation, and cancer. *Cell* 140:883–899. <http://dx.doi.org/10.1016/j.cell.2010.01.025>.
5. Terzic J, Grivninkov S, Karin E, Karin M. 2010. Inflammation and colon cancer. *Gastroenterology* 138:2101–2114. <http://dx.doi.org/10.1053/j.gastro.2010.01.058>.
6. Abt MC, Osborne LC, Monticelli LA, Doering TA, Alenghat T, Sonnenberg GF, Paley MA, Antenus M, Williams KL, Erikson J, Wherry EJ, Artis D. 2012. Commensal bacteria calibrate the activation threshold of innate antiviral immunity. *Immunity* 37:158–170. <http://dx.doi.org/10.1016/j.immuni.2012.04.011>.
7. McAleer JP, Kolls JK. 2012. Maintaining poise: commensal microbiota calibrate interferon responses. *Immunity* 37:10–12. <http://dx.doi.org/10.1016/j.immuni.2012.07.001>.
8. Santaolalla R, Abreu MT. 2012. Innate immunity in the small intestine. *Curr Opin Gastroenterol* 28:124–129. <http://dx.doi.org/10.1097/MOG.0b013e3283506559>.
9. Santos RL, Raffatellu M, Bevins CL, Adams LG, Tukul C, Tsolis RM, Baumler AJ. 2009. Life in the inflamed intestine, Salmonella style. *Trends Microbiol* 17:498–506. <http://dx.doi.org/10.1016/j.tim.2009.08.008>.
10. Plataniias LC. 2005. Mechanisms of type-I- and type-II-interferon-mediated signalling. *Nat Rev Immunol* 5:375–386. <http://dx.doi.org/10.1038/nri1604>.
11. Kole A, He J, Rivollier A, Silveira DD, Kitamura K, Maloy KJ, Kelsall BL. 2013. Type I IFNs regulate effector and regulatory T cell accumulation and anti-inflammatory cytokine production during T cell-mediated colitis. *J Immunol* 191:2771–2779. <http://dx.doi.org/10.4049/jimmunol.1301093>.
12. Lienenklaus S, Cornitescu M, Zietara N, Lyszkiewicz M, Gekara N, Jablonska J, Edenhofer F, Rajewsky K, Bruder D, Hafner M, Staeheli P, Weiss S. 2009. Novel reporter mouse reveals constitutive and inflammatory expression of IFN-beta *in vivo*. *J Immunol* 183:3229–3236. <http://dx.doi.org/10.4049/jimmunol.0804277>.
13. Fuchs SY. 2013. Hope and fear for interferon: the receptor-centric outlook on the future of interferon therapy. *J Interferon Cytokine Res* 33:211–225. <http://dx.doi.org/10.1089/jir.2012.0117>.
14. Piehler J, Thomas C, Garcia KC, Schreiber G. 2012. Structural and dynamic determinants of type I interferon receptor assembly and their functional interpretation. *Immunol Rev* 250:317–334. <http://dx.doi.org/10.1111/imr.12001>.
15. Uze G, Schreiber G, Piehler J, Pellegrini S. 2007. The receptor of the type I interferon family. *Curr Top Microbiol Immunol* 316:71–95.
16. Tschurtschenthaler M, Wang J, Fricke C, Fritz TM, Niederreiter L, Adolph TE, Sarcevic E, Kunzel S, Offner FA, Kalinke U, Baines JF, Tilg H, Kaser A. 2014. Type I interferon signalling in the intestinal epithelium affects Paneth cells, microbial ecology and epithelial regeneration. *Gut* 63:1921–1931. <http://dx.doi.org/10.1136/gutjnl-2013-305863>.
17. Rauch I, Hainzl E, Rosebrock F, Heider S, Schwab C, Berry D, Stoiber D, Wagner M, Schleper C, Loy A, Urich T, Muller M, Strobl B, Kenner L, Decker T. 2014. Type I interferons have opposing effects during the emergence and recovery phases of colitis. *Eur J Immunol* 44:2749–2760. <http://dx.doi.org/10.1002/eji.201344401>.
18. Sun L, Miyoshi H, Origanti S, Nice TJ, Barger AC, Manieri NA, Fogel LA, French AR, Pivnicka-Worms D, Pivnicka-Worms H, Virgin HW, Lenschow DJ, Stappenbeck TS. 2015. Type I interferons link viral infection to enhanced epithelial turnover and repair. *Cell Host Microbe* 17:85–97. <http://dx.doi.org/10.1016/j.chom.2014.11.004>.
19. Levin D, Harari D, Schreiber G. 2011. Stochastic receptor expression determines cell fate upon interferon treatment. *Mol Cell Biol* 31:3252–3266. <http://dx.doi.org/10.1128/MCB.05251-11>.
20. Kumar KG, Barriere H, Carbone CJ, Liu J, Swaminathan G, Xu P, Li Y, Baker DP, Peng J, Lukacs GL, Fuchs SY. 2007. Site-specific ubiquitination exposes a linear motif to promote interferon-alpha receptor endocytosis. *J Cell Biol* 179:935–950. <http://dx.doi.org/10.1083/jcb.200706034>.
21. Kumar KG, Krolewski JJ, Fuchs SY. 2004. Phosphorylation and specific ubiquitin acceptor sites are required for ubiquitination and degradation of the IFNAR1 subunit of type I interferon receptor. *J Biol Chem* 279:46614–46620. <http://dx.doi.org/10.1074/jbc.M407082200>.
22. Kumar KG, Tang W, Ravindranath AK, Clark WA, Croze E, Fuchs SY. 2003. SCF(HOS) ubiquitin ligase mediates the ligand-induced down-regulation of the interferon-alpha receptor. *EMBO J* 22:5480–5490. <http://dx.doi.org/10.1093/emboj/cdg524>.
23. Liu J, Plotnikov A, Banerjee A, Suresh Kumar KG, Ragimbeau J, Marjanovic Z, Baker DP, Pellegrini S, Fuchs SY. 2008. Ligand-independent pathway that controls stability of interferon alpha receptor. *Biochem Biophys Res Commun* 367:388–393. <http://dx.doi.org/10.1016/j.bbrc.2007.12.137>.
24. Zheng H, Qian J, Baker DP, Fuchs SY. 2011. Tyrosine phosphorylation of protein kinase D2 mediates ligand-inducible elimination of the type I

- interferon receptor. *J Biol Chem* 286:35733–35741. <http://dx.doi.org/10.1074/jbc.M111.263608>.
25. Zheng H, Qian J, Varghese B, Baker DP, Fuchs S. 2011. Ligand-stimulated downregulation of the alpha interferon receptor: role of protein kinase D2. *Mol Cell Biol* 31:710–720. <http://dx.doi.org/10.1128/MCB.01154-10>.
  26. Liu J, HuangFu WC, Kumar KG, Qian J, Casey JP, Hamanaka RB, Grigoriadou C, Aldabe R, Diehl JA, Fuchs SY. 2009. Virus-induced unfolded protein response attenuates antiviral defenses via phosphorylation-dependent degradation of the type I interferon receptor. *Cell Host Microbe* 5:72–83. <http://dx.doi.org/10.1016/j.chom.2008.11.008>.
  27. Huangfu WC, Qian J, Liu C, Liu J, Lokshin AE, Baker DP, Rui H, Fuchs SY. 2012. Inflammatory signaling compromises cell responses to interferon alpha. *Oncogene* 31:161–172. <http://dx.doi.org/10.1038/onc.2011.221>.
  28. Bhattacharya S, Katlinski KV, Reichert M, Takano S, Brice A, Zhao B, Yu Q, Zheng H, Carbone CJ, Katlinskaya YV, Leu NA, McCorkell KA, Srinivasan S, Gironde M, Rui H, May MJ, Avadhani NG, Rustgi AK, Fuchs SY. 2014. Triggering ubiquitination of IFNAR1 protects tissues from inflammatory injury. *EMBO Mol Med* 6:384–397. <http://dx.doi.org/10.1002/emmm.201303236>.
  29. Liu J, Carvalho LP, Bhattacharya S, Carbone CJ, Kumar KG, Leu NA, Yau PM, Donald RG, Weiss MJ, Baker DP, McLaughlin KJ, Scott P, Fuchs SY. 2009. Mammalian casein kinase 1alpha and its leishmanial ortholog regulate stability of IFNAR1 and type I interferon signaling. *Mol Cell Biol* 29:6401–6412. <http://dx.doi.org/10.1128/MCB.00478-09>.
  30. Amit S, Hatzubai A, Birman Y, Andersen JS, Ben-Shushan E, Mann M, Ben-Neriah Y, Alkalay I. 2002. Axin-mediated CKI phosphorylation of beta-catenin at Ser 45: a molecular switch for the Wnt pathway. *Genes Dev* 16:1066–1076. <http://dx.doi.org/10.1101/gad.230302>.
  31. Liu C, Li Y, Semenov M, Han C, Baeg GH, Tan Y, Zhang Z, Lin X, He X. 2002. Control of beta-catenin phosphorylation/degradation by a dual-kinase mechanism. *Cell* 108:837–847. [http://dx.doi.org/10.1016/S0092-8674\(02\)00685-2](http://dx.doi.org/10.1016/S0092-8674(02)00685-2).
  32. Fuchs SY, Chen A, Xiong Y, Pan ZQ, Ronai Z. 1999. HOS, a human homolog of Slimb, forms an SCF complex with Skp1 and Cullin1 and targets the phosphorylation-dependent degradation of IkappaB and beta-catenin. *Oncogene* 18:2039–2046. <http://dx.doi.org/10.1038/sj.onc.1202760>.
  33. Hart M, Concordet JP, Lassot I, Albert I, del los Santos R, Durand H, Perret C, Rubinfeld B, Margottin F, Benarous R, Polakis P. 1999. The F-box protein beta-TrCP associates with phosphorylated beta-catenin and regulates its activity in the cell. *Curr Biol* 9:207–210. [http://dx.doi.org/10.1016/S0960-9822\(99\)80091-8](http://dx.doi.org/10.1016/S0960-9822(99)80091-8).
  34. Kitagawa M, Hatakeyama S, Shirane M, Matsumoto M, Ishida N, Hattori K, Nakamichi I, Kikuchi A, Nakayama K, Nakayama K. 1999. An F-box protein, FWD1, mediates ubiquitin-dependent proteolysis of beta-catenin. *EMBO J* 18:2401–2410. <http://dx.doi.org/10.1093/emboj/18.9.2401>.
  35. Latres E, Chiaur DS, Pagano M. 1999. The human F box protein beta-Trcp associates with the Cull1/Skp1 complex and regulates the stability of beta-catenin. *Oncogene* 18:849–854. <http://dx.doi.org/10.1038/sj.onc.1202653>.
  36. Winston JT, Strack P, Beer-Romero P, Chu CY, Elledge SJ, Harper JW. 1999. The SCFbeta-TRCP-ubiquitin ligase complex associates specifically with phosphorylated destruction motifs in IkappaBalpha and beta-catenin and stimulates IkappaBalpha ubiquitination in vitro. *Genes Dev* 13:270–283. <http://dx.doi.org/10.1101/gad.13.3.270>.
  37. Elyada E, Pribluda A, Goldstein RE, Morgenstern Y, Brachya G, Cojocaru G, Snir-Alkalay I, Burstain I, Haffner-Krausz R, Jung S, Wiener Z, Alitalo K, Oren M, Pikarsky E, Ben-Neriah Y. 2011. CK1alpha ablation highlights a critical role for p53 in invasiveness control. *Nature* 470:409–413. <http://dx.doi.org/10.1038/nature09673>.
  38. Pribluda A, Elyada E, Wiener Z, Hamza H, Goldstein RE, Biton M, Burstain I, Morgenstern Y, Brachya G, Billauer H, Biton S, Snir-Alkalay I, Vucic D, Schlereth K, Mernberger M, Stiewe T, Oren M, Alitalo K, Pikarsky E, Ben-Neriah Y. 2013. A senescence-inflammatory switch from cancer-inhibitory to cancer-promoting mechanism. *Cancer Cell* 24:242–256. <http://dx.doi.org/10.1016/j.ccr.2013.06.005>.
  39. Greten FR, Eckmann L, Greten TF, Park JM, Li ZW, Egan LJ, Kagnoff MF, Karin M. 2004. IKKbeta links inflammation and tumorigenesis in a mouse model of colitis-associated cancer. *Cell* 118:285–296. <http://dx.doi.org/10.1016/j.cell.2004.07.013>.
  40. Katlinskaya YV, Carbone CJ, Yu Q, Fuchs SY. 2015. Type 1 interferons contribute to the clearance of senescent cell. *Cancer Biol Ther* 16:1214–1219. <http://dx.doi.org/10.1080/15384047.2015.1056419>.
  41. Sato T, Vries RG, Snippert HJ, van de Wetering M, Barker N, Stange DE, van Es JH, Abo A, Kujala P, Peters PJ, Clevers H. 2009. Single Lgr5 stem cells build crypt-villus structures in vitro without a mesenchymal niche. *Nature* 459:262–265. <http://dx.doi.org/10.1038/nature07935>.
  42. Yu Q, Carbone CJ, Katlinskaya YV, Zheng H, Zheng K, Luo M, Wang PJ, Greenberg RA, Fuchs SY. 2015. Type I interferon controls propagation of long interspersed element-1. *J Biol Chem* 290:10191–10199. <http://dx.doi.org/10.1074/jbc.M114.612374>.
  43. Yu Q, Katlinskaya YV, Carbone CJ, Zhao B, Katlinski KV, Zheng H, Guha M, Li N, Chen Q, Yang T, Lengner CJ, Greenberg RA, Johnson FB, Fuchs SY. 2015. DNA-damage-induced type I interferon promotes senescence and inhibits stem cell function. *Cell Rep* 11:785–797. <http://dx.doi.org/10.1016/j.celrep.2015.03.069>.
  44. Moiseeva O, Mallette FA, Mukhopadhyay UK, Moores A, Ferbeyre G. 2006. DNA damage signaling and p53-dependent senescence after prolonged beta-interferon stimulation. *Mol Biol Cell* 17:1583–1592. <http://dx.doi.org/10.1091/mbc.E05-09-0858>.
  45. Wong MH, Rubinfeld B, Gordon JI. 1998. Effects of forced expression of an NH2-terminal truncated beta-catenin on mouse intestinal epithelial homeostasis. *J Cell Biol* 141:765–777. <http://dx.doi.org/10.1083/jcb.141.3.765>.
  46. Sansom OJ, Reed KR, Hayes AJ, Ireland H, Brinkmann H, Newton IP, Battle E, Simon-Assmann P, Clevers H, Nathke IS, Clarke AR, Winton DJ. 2004. Loss of Apc in vivo immediately perturbs Wnt signaling, differentiation, and migration. *Genes Dev* 18:1385–1390. <http://dx.doi.org/10.1101/gad.287404>.
  47. Mangan NE, Fung KY. 2012. Type I interferons in regulation of mucosal immunity. *Immunol Cell Biol* 90:510–519. <http://dx.doi.org/10.1038/icb.2012.13>.
  48. Knippschild U, Gocht A, Wolff S, Huber N, Lohler J, Stoter M. 2005. The casein kinase 1 family: participation in multiple cellular processes in eukaryotes. *Cell Signal* 17:675–689. <http://dx.doi.org/10.1016/j.cellsig.2004.12.011>.
  49. Takaoka A, Hayakawa S, Yanai H, Stoiber D, Negishi H, Kikuchi H, Sasaki S, Imai K, Shibue T, Honda K, Taniguchi T. 2003. Integration of interferon-alpha/beta signalling to p53 responses in tumour suppression and antiviral defence. *Nature* 424:516–523. <http://dx.doi.org/10.1038/nature01850>.
  50. Preitner N, Quan J, Nowakowski DW, Hancock ML, Shi J, Tcherkezian J, Young-Pearse TL, Flanagan JG. 2014. APC is an RNA-binding protein, and its interactome provides a link to neural development and microtubule assembly. *Cell* 158:368–382. <http://dx.doi.org/10.1016/j.cell.2014.05.042>.
  51. Valvezan AJ, Huang J, Lengner CJ, Pack M, Klein PS. 2014. Oncogenic mutations in adenomatous polyposis coli (Apc) activate mechanistic target of rapamycin complex 1 (mTORC1) in mice and zebrafish. *Dis Model Mech* 7:63–71. <http://dx.doi.org/10.1242/dmm.012625>.
  52. Wang S, Li N, Yousefi M, Nakauka-Ddamba A, Li F, Parada K, Rao S, Minuesa G, Katz Y, Gregory BD, Kharas MG, Yu Z, Lengner CJ. 2015. Transformation of the intestinal epithelium by the MSI2 RNA-binding protein. *Nat Commun* 6:6517. <http://dx.doi.org/10.1038/ncomms7517>.
  53. Katakura K, Lee J, Rachmilewitz D, Li G, Eckmann L, Raz E. 2005. Toll-like receptor 9-induced type I IFN protects mice from experimental colitis. *J Clin Invest* 115:695–702. <http://dx.doi.org/10.1172/JCI22996>.
  54. Jostins L, Ripke S, Weersma RK, Duerr RH, McGovern DP, Hui KY, Lee JC, Schumm LP, Sharma Y, Anderson CA, Essers J, Mitrovic M, Ning K, Cleynen I, Theatre E, Spain SL, Raychaudhuri S, Goyette P, Wei Z, Abraham C, Achkar JP, Ahmad T, Amininejad L, Ananthakrishnan AN, Andersen V, Andrews JM, Baidoo L, Balschun T, Bampton PA, Bitton A, Boucher G, Brand S, Buning C, Cohain A, Cichon S, D'Amato M, De Jong D, Devaney KL, Dubinsky M, Edwards C, Ellinghaus D, Ferguson LR, Franchimont D, Fransen K, Geary R, Georges M, Gieger C, Glas J, Haritunians T, Hart A, et al. 2012. Host-microbe interactions have shaped the genetic architecture of inflammatory bowel disease. *Nature* 491:119–124. <http://dx.doi.org/10.1038/nature11582>.
  55. Gonzalez-Navajas JM, Lee J, David M, Raz E. 2012. Immunomodulatory functions of type I interferons. *Nat Rev Immunol* 12:125–135. <http://dx.doi.org/10.1038/nri3133>.